NASA CONTRACTOR REPORT

NASA CR-1956

SOME EFFECTS OF SWIRL ON TURBULENT MIXING AND COMBUSTION

by Arthur Rubel

Prepared by
ADVANCED TECHNOLOGY LABORATORIES, INC.
Jericho, N.Y. 11753
for

NATIONAL AERONAUTICS AND SPACE ADMINISTRATION • WASHINGTON, D. C. • FEBRUARY 1972

1. Report No. NASA CR-1956	2. Government Accession No.	3. Recipient's Catalog No.
4. Title and Subtitle SOME EFFECTS OF SWIRL ON TURBULENT MIXING AND COMBUSTION		5. Report Date February 1972 6. Performing Organization Code
7. Author(s) Arthur Rubel		8. Performing Organization Report No. ATLI ATL TR 162
9. Performing Organization Name and Address Advanced Technology Laboratories, Inc. 400 Jericho Turnpike Jericho, N. Y. 11753		10. Work Unit No. 11. Contract or Grant No. NASW-2075
12. Sponsoring Agency Name and Address National Aeronautics and Space Administration Washington, D. C.		13. Type of Report and Period Covered Contractor Report 14. Sponsoring Agency Code RAA
15. Supplementary Notes		

16. Abstract

A general formulation of some effects of swirl on turbulent mixing is given. The basis for the analysis is that momentum transport is enhanced by turbulence resulting from rotational instability of the fluid field.

An appropriate form for the turbulent eddy viscosity is obtained by mixing length type arguments. The result takes the form of a corrective factor that is a function of the swirl and acts to increase the eddy viscosity. The factor is based upon the initial mixing conditions implying that the rotational turbulence decays in a manner similar to that of free shear turbulence.

Existing experimental data for free jet combustion are adequately matched by using the factor $(1 + 90/N_{Ro}^2)^{\frac{1}{2}}$ to relate the effects of swirl on eddy viscosity.

The model is extended and applied to the supersonic combustion of a ring jet of hydrogen injected into a constant area annular air stream. The computations demonstrate that swirling the flow could

(1) reduce the burning length by one half
(2) result in more uniform burning across the annulus width
(3) open the possibility of optimization of the combustion characteristics by locating the fuel jet between the inner wall and center of the annulus width.

17. Key Words (Suggested by Author(s))	18. Distribution Statement
Turbulent Mixing Combustion Swirl Combustors	Unclassified - Unlimited

19. Security Classif. (of this report)	20. Security Classif. (of this page)	21. No. of Pages	22. Price*
Unclassified	Unclassified	58	$3.00

*For sale by the National Technical Information Service, Springfield, Virginia 22151

1. Jet mixing flows
2. Turbulent flows
3. Combustion

247172

TABLE OF CONTENTS

LIST OF FIGURES

LIST OF FIGURES (Continued)

LIST OF TABLES

LIST OF SYMBOLS

a	speed of sound
C	constant described in Equation (12)
c_f	skin friction coefficient
$\bar{C}_P$	mixture specific heat at constant pressure
C_{P_k}	specific heat at constant pressure for species k
D_T	turbulent diffusion coefficient
h_k	specific enthalpy of species k
H	mixture specific total enthalpy
K_T	turbulent thermal conductivity
K	constant defined in Equation (15)
ℓ	mixing length
L	reference length
L_s	length for flame stabilization as per Reference (3)
L_f	flame length
m	number of elemental species
M_k	molecular weight of species k
n	number of chemical species
N_{Le}	Lewis number; $\rho D_T/\mu_T$
N_M	Mach number; u/a
N_{Pr}	Prandtl number; $\mu_T \bar{C}p/K_T$
N_{Re}	Reynolds number; $\rho_j u_j r_j/\mu_T$
N_{Ro}	Rossby number; u/W
p	pressure
r	radial coordinate
$r_{\frac{1}{2}}$	half radius; where $u=\frac{1}{2}(u_e+u_a)$
R	universal gas constant
S	degree of swirl; $\int_0^{r_j} \rho u w r^2 dr \Big/ r_j \int_0^{r_j} \rho u^2 r dr$

T	temperature
u	axial velocity
v	radial velocity
w	tangential (swirl) velocity
$\dot{w}_k$	mass rate of production of species k
x	axial coordinate
α_k	mass fraction of chemical species k
$\tilde{\alpha}_k$	mass fraction of elemental species k
Δr_j	width of ring jet
ε	eddy kinematic viscosity
κ	constant defined in Equation (34)
μ_T	turbulent (eddy) viscosity
ρ	density
ϕ	equivalence ratio
ψ	stream function

SUPERSCRIPTS

$'$	turbulent fluctuation
$\bar{}$	averaged quantity

SUBSCRIPTS

a	axis
e	edge or outer wall
i	inner wall
j	jet

ACKNOWLEDGEMENT

This work was performed by Advanced Technology Laboratories, Inc., for the National Aeronautics and Space Administration under Contract No. NASW-2075.

The author is grateful to Dr. Antonio Ferri for many productive discussions that aided in the formulation and interpretation of this problem, and to Dr. Paolo Baronti for his many valuable criticisms during the course of this work.

I. INTRODUCTION

It has long been known that the introduction of swirl to a flow of reacting fluids can enhance the combustion process. Schwartz's experiment, Reference (1), demonstrated that rotating a propane-air mixture in an annular combustion chamber results in appreciable shortening of the flame length, increased flame divergence, improved stability characteristics and delayed blow-off.

Swirl-can combustors presently under development, Reference (2), have also utilized fluid rotation as well as special geometric configurations to achieve greater combustion stability.

Detailed measurements of the properties of a turbulent jet diffusion flame with swirl have been given by Chervinsky, Reference (3). Here too, a shortening of the stabilization and flame lengths with increased swirl is observed. An accompanying analysis includes a quantitative evaluation of the turbulent eddy viscosity and Prandtl number from the experimental data for three different degrees of swirl.

Although improved characteristics of mixing and combustion with swirl have been observed, the basic causes of this phenomenon are not well understood. A purpose of this re-

port is to present a model that accounts for some of the effects of swirl as a consequence of the rotational instability created by its introduction into the flow.

Mixing length concepts are utilized to demonstrate that the addition of a swirl component to the flow enhances the turbulent transport of momentum. The improved transport is evidenced by a modifying factor that increases the eddy viscosity as a function of swirl and density.

The model is compared with the three experiments of Reference (3) concerning the combustion of a free jet in a quiescent medium. It is shown that the formulation

$$\mu_T \alpha (1+90/N_{Ro}^2)^{\frac{1}{2}} \rho_j u_j r_j \qquad (1)$$

is in good agreement with that data over the range of swirl presented.

In order to extend these results to the case of free jet combustion in a uniformly moving medium, a computer program was developed to solve the governing fluid dynamic equations with a flame sheet model incorporated to describe the combustion process. After demonstrating that these results collapse to the quiescent medium case for low edge velocities, it is

found that the eddy viscosity for the jet in a uniformly moving medium is modified in a manner similar to that for the quiescent medium.

Since the eddy viscosity model given here implies rapid mixing when swirl is introduced to the injected fuel, applications to confined supersonic combustion are apparent. To quantitatively evaluate the effects of swirl on supersonic combustion a computer program was developed to calculate the finite rate combustion of hydrogen injected from a ring jet into an air stream in an annular channel.

Although mixing is even more rapid for a heavier fuel, hydrogen was chosen because its chemistry is well known. Even for the hydrogen case the results of this study show that the introduction of swirl to the fuel jet can reduce the combustor length by one half and result in more uniform burning across the width of the annulus.

It is planned to extend the current results and apply them to a variety of new combustor schemes.

II. TURBULENT MIXING MODEL

A physical description of the instability of a flow field is often given as follows. If a fluid particle is removed from its initial position to some other one in the flow field, then the background field is stable if a restoring force is exerted on the fluid particle. The background field is unstable if a force tends to move the particle further away from its origin and neutrally stable if no net force is exerted on the particle.

For an axisymmetric flow field with rotational motion this concept is easily put in terms of the parameters of that field. As shown in Figure (1), a fluid particle originating from radius r_1 with density ρ_1, swirl velocity w_1 is considered to have been displaced to a position at r_2. If it is assumed that the process is adiabatic and that the radial pressure differences play an insignificant role in determining local density differences, then the density of the particle remains unchanged at its new position. Since there is no torque exerted on the particle its angular momentum is constant so that the swirl velocity at the new position must be given by

$$w_1' = \frac{r_1 w_1}{r_2}.$$

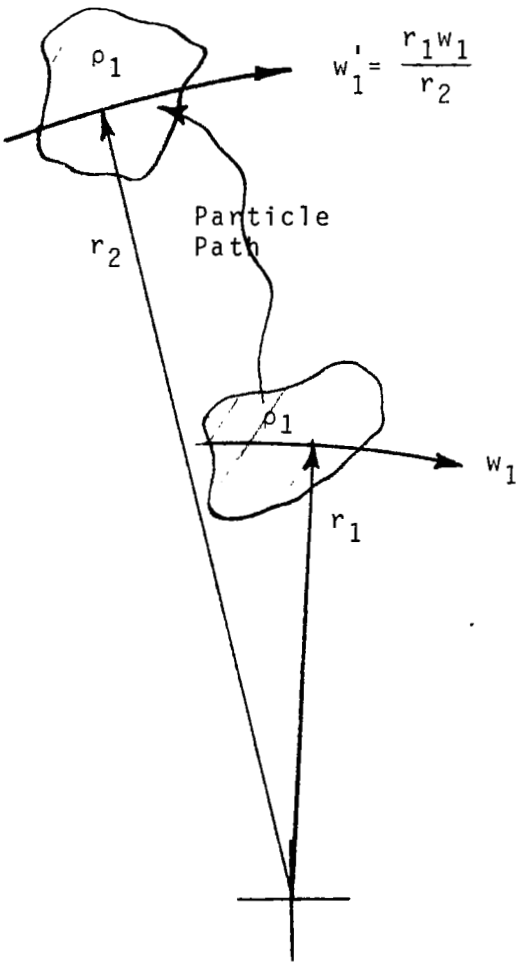

FIGURE 1. FLUID PARTICLE DISPLACEMENT IN SWIRL FLOW FIELD

The pressure gradient required to balance the centrifugal force of the particle at r_2 is given by the equation of radial equilibrium

$$\left(\frac{dp}{dr}\right)^* = \frac{\rho_1 (w_1')^2}{r_2} = \frac{\rho_1 r_1^2 w_1^2}{r_2^3} . \tag{2}$$

The existing flow field, however, has impressed a pressure gradient on the particle given by

$$\left(\frac{dp}{dr}\right)_2 = \frac{\rho_2 w_2^2}{r_2} \tag{3}$$

Thus, in order for a net restoring force to be exerted on the particle, and stability of the rotational flow field,

$$\left(\frac{dp}{dr}\right)_2 > \left(\frac{dp}{dr}\right)^* \Longrightarrow \rho_2 w_2^2 r_2^2 > \rho_1 w_1^2 r_1^2 \tag{4}$$

This condition, for constant density, was first given by Rayleigh, Reference (4), whereas the above physical descrip-

tion has been attributed in Reference (5) to von Kármán, Reference (6). A mathematical basis for these results has been provided in Reference (7) by Synge who arrived at the criterion

$$\frac{d}{dr}\left(\rho r^2 w^2\right) \begin{cases} > \\ = \\ < \end{cases} 0 \qquad \begin{matrix} \text{Stable} \\ \text{Neutral} \\ \text{Unstable} \end{matrix} \tag{5}$$

A motion that is rotationally unstable can result in a state of greater turbulence exhibiting increased transport properties. In order to determine the effects of rotational instability on the eddy kinematic viscosity, some essential features of the Prandtl mixing length theory in a non-rotating field are reviewed from Reference (8).

The eddy kinematic viscosity, ε, is defined by

$$\varepsilon \frac{d\bar{u}}{dr} \equiv \overline{u'v'} \tag{6}$$

in the case where transport of axial velocity in the normal (radial) direction is being considered. If it is assumed that the fluctuating components of velocity indicated by the

primed quantities, are of the same order, then

$$\varepsilon \frac{d\bar{u}}{dr} \alpha |\bar{u}'| . |\bar{v}'| \quad \alpha |\bar{u}'| \; |\bar{u}'| . \tag{7}$$

As a result of Prandtl's mixing length hypothesis

$$|\bar{u}'| \cdot |\bar{u}'| \quad \alpha \quad \bar{\ell}^2 \left(\frac{d\bar{u}}{dr} \right)^2 \tag{8}$$

when ℓ is the Prandtl mixing length.

Combining Equations (7) and (8) the Prandtl formulation for eddy viscosity is obtained

$$\varepsilon \alpha \bar{\ell}^2 \frac{d\bar{u}}{dr} . \tag{9}$$

The eddy kinematic velocity may then be written in terms of a turbulent energy transfer as

$$\varepsilon^2 \alpha \bar{\ell}^2 \overline{u'^2} \tag{10}$$

This formulation proves useful for developing arguments on the effects of rotational instability on the turbulent viscosity.

In a rotationally unstable flow the centrifugal force per unit mass impressed upon an eddy is

$$\frac{(\rho w^2)'}{\rho r}.$$

If it is assumed that this eddy travels a distance ℓ' before it arrives at the reference radius then the work done will be proportional to

$$\frac{\ell'(\rho w^2)'}{\rho r}.$$

Utilizing mixing length concepts, this expression may be arranged in terms of the gradients of the mean background flow so that the energy transported due to the rotational instability is

$$\overline{[\bar{\ell}^2 w'^2]}_{\substack{\text{rot.} \\ \text{inst.}}} \alpha\ \bar{\ell}^2\ \overline{\frac{\ell'(\rho w^2)'}{\rho r}}\ \alpha\ \frac{\bar{\ell}^4}{\rho r}\ \frac{\partial \overline{\rho w^2}}{\partial r}. \qquad (11)$$

An argument based upon average velocities of mixing (turbulent fluctuations) can also be given. In principle, it is identical to the previous argument but here the details will be more apparent.

Suppose we look at the radius r_o of the turbulent flow field and find some fluid particles moving outward and some inward in an eddy-like motion as shown in Figure (2).

The driving forces on two oppositely moving fluid particles should be proportional to the difference between the pressure and centrifugal forces. Thus,

$$F_1 \propto \frac{(\rho_1 w_1^2 - \rho_o w_o^2)}{r_o}, \quad F_2 \propto \frac{(\rho_2 w_2^2 - \rho_o w_o^2)}{r_o}.$$

Assuming the same proportionality, then from Newton's second law an expression for the average relative velocity between the two particles may be given by

$$\overline{\frac{d}{dt}(v_1 - v_2)} = \overline{\frac{dv_r}{dt}} = \overline{v_r \frac{\partial v_r}{\partial r}} \propto \overline{\frac{\Delta_1 \rho w^2}{r_o \rho_1} - \frac{\Delta_2 \rho w}{r_o \rho_2}}$$

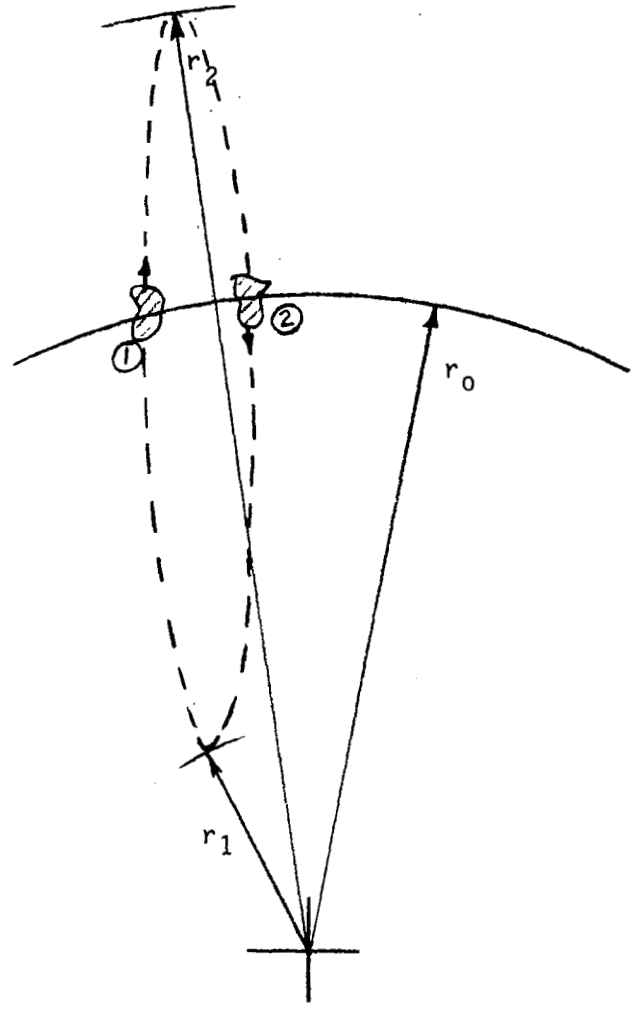

FIGURE 2. ROTATIONALLY UNSTABLE EDDY MOTION

Integrating over some appropriate mixing length, ℓ, and replacing the relative velocity by the turbulent fluctuation then

$$\frac{\overline{v'^2}}{2} \quad \alpha \quad \overline{\int_o^{\ell} \left(\frac{\Delta_1 \rho w^2}{r_o \rho_1} - \frac{\Delta_2 \rho w^2}{r_o \rho_2} \right) dr}.$$

To first order this may be written as

$$\overline{v'^2} \quad \alpha \quad \frac{\overline{(\rho_1 w_1^2 - \rho_2 w_2^2)}}{\rho_o r_o} \ell \quad \alpha \quad \frac{\overline{\ell}^2}{\rho_o r_o} \frac{\partial \overline{\rho w^2}}{\partial r}$$

which is in agreement with the previous result given by Equation (11).

These results for the effect of rotational instability on turbulent energy transport may now be incorporated into the eddy kinematic viscosity model. Adding the energy transport from rotation effects from Equation (11) to the transport from usual shear effects from Equation (8) results in

$$\left(\overline{\ell}^2 \overline{u'^2} \right)_{shear} + \left(\overline{\ell}^2 \overline{w'^2} \right)_{rot.} \quad \alpha \quad \overline{\ell}^4 \left[\left(\frac{d\overline{u}}{dr} \right)^2 + \frac{C}{\rho r} \frac{d\overline{\rho w^2}}{dr} \right] \qquad (12)$$

Where C is some constant representing the relative magnitudes of the two effects. This constant must be determined by experiment.

An equation for the eddy kinematic viscosity is found from Equations (10) and (12)

$$\varepsilon \quad \alpha \quad \bar{\ell}^2 \left[\left(\frac{d\bar{u}}{dr} \right)^2 + \frac{C}{\rho r} \left| \frac{\overline{d\rho w^2}}{dr} \right| \right]^{1/2} . \tag{13}$$

The quantity $\frac{d(\rho w^2)}{dr}$ may be written as

$$\frac{d\rho w^2}{dr} = \frac{1}{r^2} \frac{d}{dr} (\rho r^2 w^2) - 2 \frac{\rho w^2}{r} \tag{14}$$

Since the unstable region requires that $\frac{d}{dr} (pr^2w^2) < 0$, then it follows from Equation (14) that $\frac{d}{dr} (pw^2) < 0$.

For this reason the absolute sign appears about this quantity in Equation (13). It should be noted that for rotationally stable flows there is the possibility that the turbulent transport properties of the fluid field can be reduced from those of a comparable non-rotating fluid.

For free shear turbulence it has been suggested, Reference (8), that overall differences within the flow are more significant than local gradients. If this approach is used here then Equation (13) can be expressed as

$$\varepsilon = KL \left[(\Delta u)^2 + C \frac{L}{\rho r} |\Delta(\rho w^2)| \right]^{1/2}$$

where L is some reference length pertinent to the given problem.

Defining the turbulent viscosity in terms of the eddy kinematic viscosity, and slight rearrangement, yields

$$\mu_T \equiv \rho\varepsilon = K \left[1 + \frac{CL}{\rho r} \frac{|\Delta(\rho w^2)|}{(\Delta u)^2} \right]^{1/2} \rho L |\Delta u| . \qquad (15)$$

The form given here is similar to that usually given for turbulent free shear flows with the exception that a correction factor,

$$\left[1 + \frac{CL}{\rho r} \frac{|\Delta(\rho w^2)|}{(\Delta u)^2} \right]^{1/2} ,$$

which includes effects of rotational instability modifies the proportionality constant, K.

III. FREE JET COMBUSTION

(a) Quiescent Medium In this section the eddy viscosity analysis that has been formulated earlier will be applied to the case of swirling free jet combustion in a quiescent medium. The consistency of that formulation with available experimental data is to be examined.

It has been shown, Reference (9), that several regimes exist for a turbulent swirling jet exhausting into a quiescent medium. As the degree of swirl is increased, the adverse pressure gradient in the area near the jet is strengthened due to the rapid decay of angular momentum. At large degrees of swirl the pressure gradient can become large enough to cause a region of reversed flow near the jet exit. Even before this condition is met the gradient can be strong enough to induce a maximum velocity at radial positions away from the axis.

The current work is concerned only with that regime of swirl such that within a small fraction of a jet radius downstream the maximum velocity appears at the axis. The objective here is to predict the effect of this low to moderate degree of swirl on the turbulent transport (eddy viscosity) within the jet combustion region. The only data available for such a correlation is that of Reference (3).

Observations, References (3) and (10), support the view that in cases such as this the swirl velocity is very quickly (~15 radii) reduced to one-tenth its original maximum quantity. Yet, the effects of swirl are seen to persist to distances of 100 diameters apparently through a lasting influence on the transport properties of the mixture. For this reason, the corrective factor for eddy viscosity of Equation (15) will be based upon initial jet conditions. Thus, for $P_e \simeq P_i$, the correcting factor can be expressed by the proportionality

$$N_{Re}^{-1} = \frac{\mu_T}{\rho_j u_j r_j} \alpha \left(1 + C \frac{w_j^2}{u_j^2}\right)^{1/2} = \left(1 + \frac{C}{N_{Ro}^2}\right)^{1/2} . \qquad (16)$$

Here, the jet radius has been used as the length parameter, while uniform axial velocity and solid body rotation have been assumed for the jet so that $\Delta\rho w^2 = (\rho w^2)$ evaluated at the jet outer edge. If the swirl distribution is not solid body then $(\rho w^2)_{max}$ should be used. The quantity u/w is often times referred to as the Rossby number. For these assumptions and near constant density in the jet the Rossby number is related to the degree of swirl by

$$2SN_{Ro} = 1. \qquad (17)$$

TABLE I

CHARACTERISTICS OF FREE JET OF REFERENCE (3)

r_j=0.082 ft, T_j=300°K, ϕ_j=5.05, P_e=2116 psf, T_e=300°K			
N_{Ro}	4.55	3.02	1.907
S	0.232	0.160	0.112
$u_{j\ max}$(ft/sec)	249.4	267.4	337.9
$w_{j\ max}$(ft/sec)	54.8	88.6	177.2
$L_{s\ exp}/r_j$	11.0	6.2	4.0
$L_{f\ calc}/r_j$	61.	38.	33.
$L_{f\ exp}/r_j$	69.	51.8	34.
$2SN_{Ro}$	1.02	0.97	0.885

Some of the data of Reference (3) is reproduced in Table I. Results have been obtained for only three values of Rossby number. The relationship given in Equation (17) is not satisfied by the case of largest swirl (N_{Ro}=1.907) probably indicating that the jet swirl did not conform to solid body rotation. The intermediate swirl case (N_{Ro}=3.02) shows the largest discrepancy between calculated and measured flame

length. For this reason, Equation (16) was matched to the eddy viscosities given for the N_{Ro}=4.55 and N_{Ro}=1.907 cases. This yields a correlation of the form

$$N_{Re}^{-1} = 0.00294\ (1 + 91.1/N_{Ro}^{2})^{1/2} \tag{18}$$

which is plotted in Figure (3) and seems to be consistent with the results of Reference (3) at all Rossby numbers. If Equation (18) is corrected for combustion gas density effects as indicated in Reference (12) then the correlation becomes

$$N_{Re}^{-1} = 0.0078\ \bar{\rho}^{1/2}\ (1 + 91.1/N_{Ro}^{2})^{1/2}$$

where $\bar{\rho}$ is the ratio of minimum combustion gas density to ambient density.

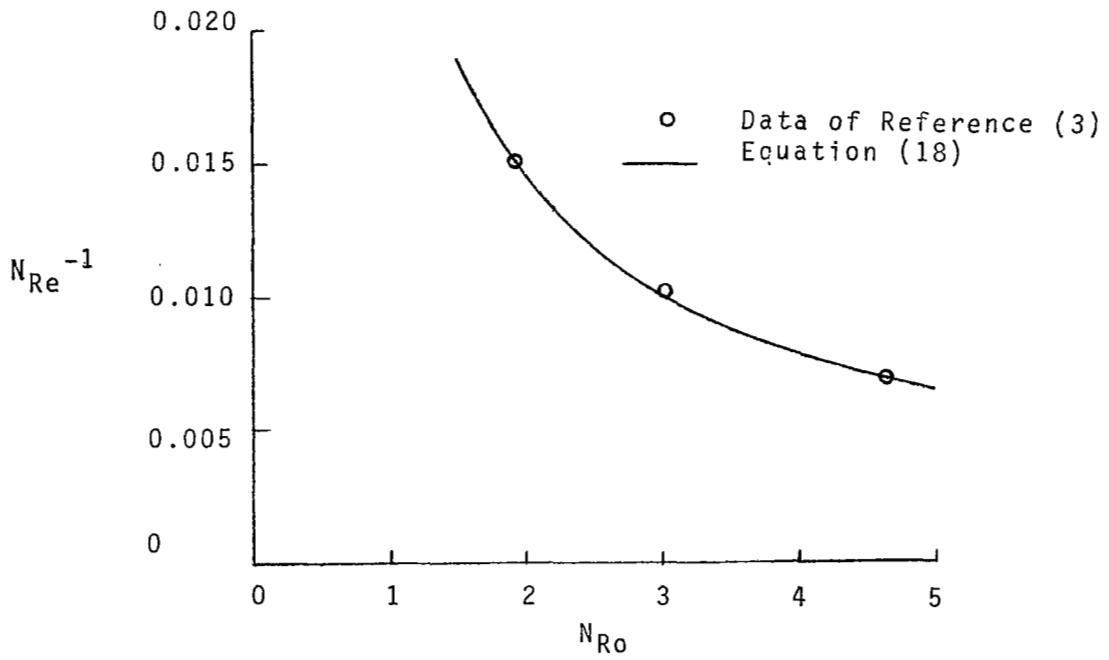

FIGURE 3. NON-DIMENSIONAL EDDY VISCOSITY (N_{Re}^{-1}) VS. ROSSBY NUMBER

(b) Uniformly Moving Medium In order to obtain another viewpoint on the free jet problem, and to gain some insight into the appropriate viscosity model for a jet exhausting into a moving external stream, a computer program was developed to solve the governing equations of the free jet system. In this system the exterior region is assumed to have a constant velocity. As this velocity is made small, the quiescent jet solution should tend to be recovered.

After applying the boundary layer approximation, the governing equations are:

Conservation of Global Mass

$$\frac{\partial}{\partial x}(\rho u r) + \frac{\partial}{\partial r}(\rho v r) = 0 \tag{19}$$

Conservation of Elemental Mass

$$\rho u \frac{\partial}{\partial x}\tilde{\alpha}_k + \rho v \frac{\partial}{\partial r}\tilde{\alpha}_k = \frac{1}{r}\frac{\partial}{\partial r}\left(\mu \frac{N_{Le}}{N_{Pr}} r \frac{\partial}{\partial r}\tilde{\alpha}_k\right), \quad k=1,m \tag{20}$$

Conservation of Axial Momentum

$$\rho u \frac{\partial u}{\partial x} + \rho v \frac{\partial u}{\partial r} = -\frac{\partial p}{\partial x} + \frac{1}{r}\frac{\partial}{\partial r}\left(\mu_T r \frac{\partial u}{\partial r}\right) \tag{21}$$

Conservation of Radial Momentum

$$\frac{\rho w^2}{r} = \frac{\partial p}{\partial r} \tag{22}$$

Conservation of Tangential Momentum

$$\rho u \frac{\partial}{\partial x}(rw) + \rho v \frac{\partial}{\partial r}(rw) = \frac{1}{r}\frac{\partial}{\partial r}\left[\mu_T\left(r\frac{\partial}{\partial r}(rw) - 2rw\right)\right] \tag{23}$$

Conservation of Energy

$$\rho u \frac{\partial H}{\partial x} + \rho v \frac{\partial H}{\partial r} = \frac{1}{r}\frac{\partial}{\partial r}\left[\mu_T r\left\{\frac{1}{N_{Pr}}\frac{\partial H}{\partial r} - \left(1 + \frac{1}{N_{Pr}}\right)\frac{w}{r}^2 + \left(1 - \frac{1}{N_{Pr}}\right)\frac{\partial(u^2/2+w^2/2)}{\partial r} + \sum_k h_k \frac{1}{N_{Pr}}(N_{Le} - 1)\frac{\partial}{\partial r}\alpha_k\right\}\right] \tag{24}$$

The chemistry of the problem is taken to be satisfied by a flame sheet model for the single step reaction of Reference (3)

$$\frac{3}{2}C_2H_6 + 5C_3H_8 + \frac{7}{2}C_4H_{10} + 53O_2 + 200\,N_2 \longrightarrow 32\,CO_2 + 42\,H_2O + 200\,N_2. \tag{25}$$

The basic assumption of this model is that at every point in the flow field the reaction is completed. Thus, in regions where the equivalence ratio, ϕ, is greater than unity only products and excess fuel are found. Similarly, wherever the equivalence ratio is less than unity only products and excess air exist. The elemental mass fractions uniquely determine the species mass fractions. The required specific enthalpies are taken as linear functions of the temperature as indicated in Table II.

TABLE II

LINEAR ENTHALPY FUNCTION OF TEMPERATURE

Species	T_k(°K)	$h_k = A_k + C_{P_k}(T-300)$ $T<T_k$		$h_k = A_k + C_{P_k}(T-2000)$ $T \geq T_k$	
		A_k (cal/gm)	C_{P_k} (cal/gm°K)	A_k (cal/gm)	C_{P_k} (cal/gm°K)
C_2H_6	0	---	---	1074.0	1.1100
C_3H_8	0	---	---	996.0	1.0980
C_4H_{10}	0	---	---	1000.0	0.9000
CO_2	762.	-2140.0	0.2020	-1640.8	0.32782
H_2O	1129.	-3205.0	0.4440	-2245.8	0.67856
O_2	905.	0.41	0.21950	442.2	0.28216
N_2	1037.	0.46	0.2490	480.0	0.3072

Application of the von Mises transformation to the governing equations arranges them into a form more amenable to numerical solution. The coordinate transformation is defined by

$$\rho ur = \psi \frac{\partial \psi}{\partial r}, \quad \rho vr = - \psi \frac{\partial \psi}{\partial x} \tag{26}$$

where

$$\psi^2 = 2 \int_o^r \rho ur' dr'.$$

This satisfies Equation (19) and recasts Equations (20) - (24) as

$$\frac{\partial \tilde{\alpha}_k}{\partial x} = \frac{1}{\psi} \frac{\partial}{\partial \psi}\left(\frac{N_{Le}}{N_{Pr}} \mu_T \frac{\rho u r^2}{\psi} \frac{\partial \tilde{\alpha}_k}{\partial \psi}\right), \quad k=1, m \tag{27}$$

$$\frac{\partial u}{\partial x} = - \frac{1}{\rho u} \frac{\partial p}{\partial x} + \frac{1}{\psi} \frac{\partial}{\partial \psi}\left(\mu_T \frac{\rho u r^2}{\psi} \frac{\partial u}{\partial \psi}\right) \tag{28}$$

$$\frac{w^2}{r^2} = \frac{u}{\psi} \frac{\partial p}{\partial \psi} \tag{29}$$

$$\frac{\partial}{\partial x} (rw) = \frac{1}{\psi} \frac{\partial}{\partial \psi}\left[\mu_T \left(\frac{\rho u r^2}{\psi} \frac{\partial}{\partial r} (rw) - 2rw\right)\right] \tag{30}$$

$$\frac{\partial H}{\partial x} = \frac{1}{\psi} \frac{\partial}{\partial \psi}\left[\mu_T \frac{\rho u r^2}{\psi}\left\{\frac{1}{N_{Pr}} \frac{\partial H}{\partial \psi} - \left(1 + \frac{1}{N_{Pr}}\right) \frac{1}{\rho} \frac{\partial p}{\partial \psi}\right.\right.$$

$$\left.\left. + \left(1 - \frac{1}{N_{Pr}}\right) \frac{\partial\left\{\frac{1}{2} (u^2+w^2)\right\}}{\partial \psi} + \sum_k h_k \frac{\left(N_{Le}-1\right)}{N_{Pr}} \frac{\partial \alpha_k}{\partial r}\right\}\right], \tag{31}$$

respectively.

The associated initial and boundary conditions for the free jet are

$$x = 0: \quad u=u_j,\ \tilde{\alpha}_k=\tilde{\alpha}_{k_j},\ H=H_j,\ w = \frac{r}{r_j} w_{max}$$

$$\psi = 0: \quad \frac{\partial u}{\partial \psi} = \frac{\partial \tilde{\alpha}_k}{\partial \psi} = \frac{\partial H}{\partial \psi} = w = 0 \tag{32}$$

$$\psi \to \infty: \quad u=u_e,\ \tilde{\alpha}_k=\tilde{\alpha}_{k_e},\ H=H_e,\ w=0,\ p=p_e$$

The above equations, along with the perfect gas law

$$p = \rho RT \sum_k \alpha_k/M_k \tag{33}$$

properly define the problem.

A straight forward explicit numerical technique was used to integrate these equations. Suffice it to say that the basic details of the numerical method can be found in Reference (13) with the following modification.

The inclusion of tangential and radial momentum equations in this analysis requires that the normal gradient of the pressure be coupled to the axial variation of the dependent variables.

This is accomplished by a simple iteration technique. First, the pressure is assumed to remain unchanged and the equations are integrated one step downstream. New values are obtained for the pressure from the latest angular momentum distribution by integrating Equation (29) from the edge value to the axis. The process is repeated until two successive iterations yield axial pressures that agreed to within 0.01 psf. In practice no more than three such iterations have ever been required and then only for the region very near the initial plane.

Before applying this analysis to the experiments of Reference (3) it is necessary to ascertain the order of the free stream velocity that is required to simulate a quiescent exterior region. Using an edge velocity of 1% of the jet velocity and the two stream eddy viscosity formulation of Kleinstein, Reference (11), a computation was made for isothermal air-air mixing. Figure (4) demonstrates that the results are in excellent agreement with the axis velocity decay profiles of References (8) and (11) indicating that a free stream velocity of the order of 1% u_j is sufficient to accurately compute axis velocity decay.

This analysis has been used to compare the limited data of Reference (3). The eddy viscosity is assumed to be of the form given by Kleinstein, neglecting the potential core and

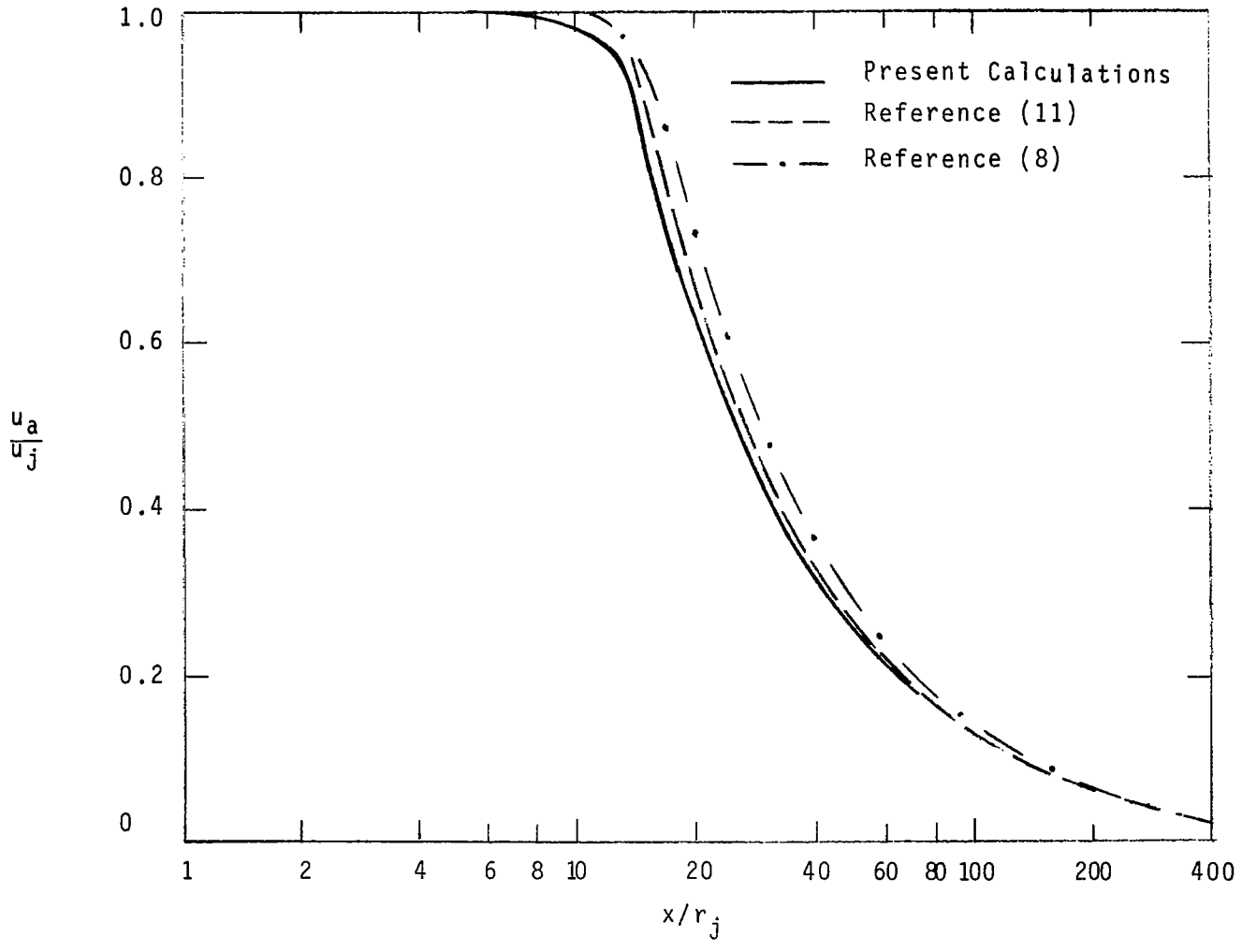

FIGURE 4. AXIAL VELOCITY DECAY AIR-AIR INJECTION

with a constant to be determined by matching the experimental data

$$\mu_T = \kappa\, r_{1/2}\, |\rho_a u_a - \rho_e u_e| \tag{34}$$

A parameter of great significance for combustor studies is the flame length and so this is the criterion that is chosen for matching the computations with κ of Equation (34). Several runs were made with initial conditions corresponding to those of Chervinsky (Table I) until the κ's for which the flame lengths were in agreement could be determined (Table III). The flame length here is defined as the distance at which the ϕ=1 line crosses the jet axis.

TABLE III

EDDY VISCOSITY CONSTANT AS FUNCTION OF ROSSBY NUMBER

N_{Ro}	4.55	3.02	1.91
κ	.0315	.044	.069

If the constant is assumed to have the same type dependence upon N_{Ro} as indicated earlier, then using the low and high N_{Ro} cases of Table III yields an eddy viscosity,

$$\mu_T = .0138 \left(1 + 88.0/N_{Ro}^2\right)^{1/2} r_{1/2} |\rho_a u_a - \rho_e u_e|. \qquad (35)$$

This result is in agreement with the variation given earlier in Equation (18). In this example it was found that $r_{\frac{1}{2}}$ should be based upon velocity and not momentum for best results. (i.e. $r_{\frac{1}{2}}$ is that value of r where $u = \frac{1}{2}(u_a+u_e)$).

Additionaly, in the current example values of $N_{Le}=1$, $N_{Pr}=0.75$ are similar to those obtained by Kleinstein in distinction from the analysis of Chevinsky. In the latter work Prandtl number was found to vary by more than two orders of magnitude through a downstream distance of 100 jet radii. Figure (5a) illustrates that the axial velocity profiles using the current matching techniques are good over a large portion of the jet decay.

The axial temperature distributions obtained, Figure (5b), are in fair agreement with those of Reference (3), but it must be recalled that a huge variation of Prandtl number was inferred from those results whereas the current computations have assumed a constant N_{Pr}. The axial temperature distributions given here have been shifted by the distance corresponding to the stabilization distance of the flame, Reference (3),

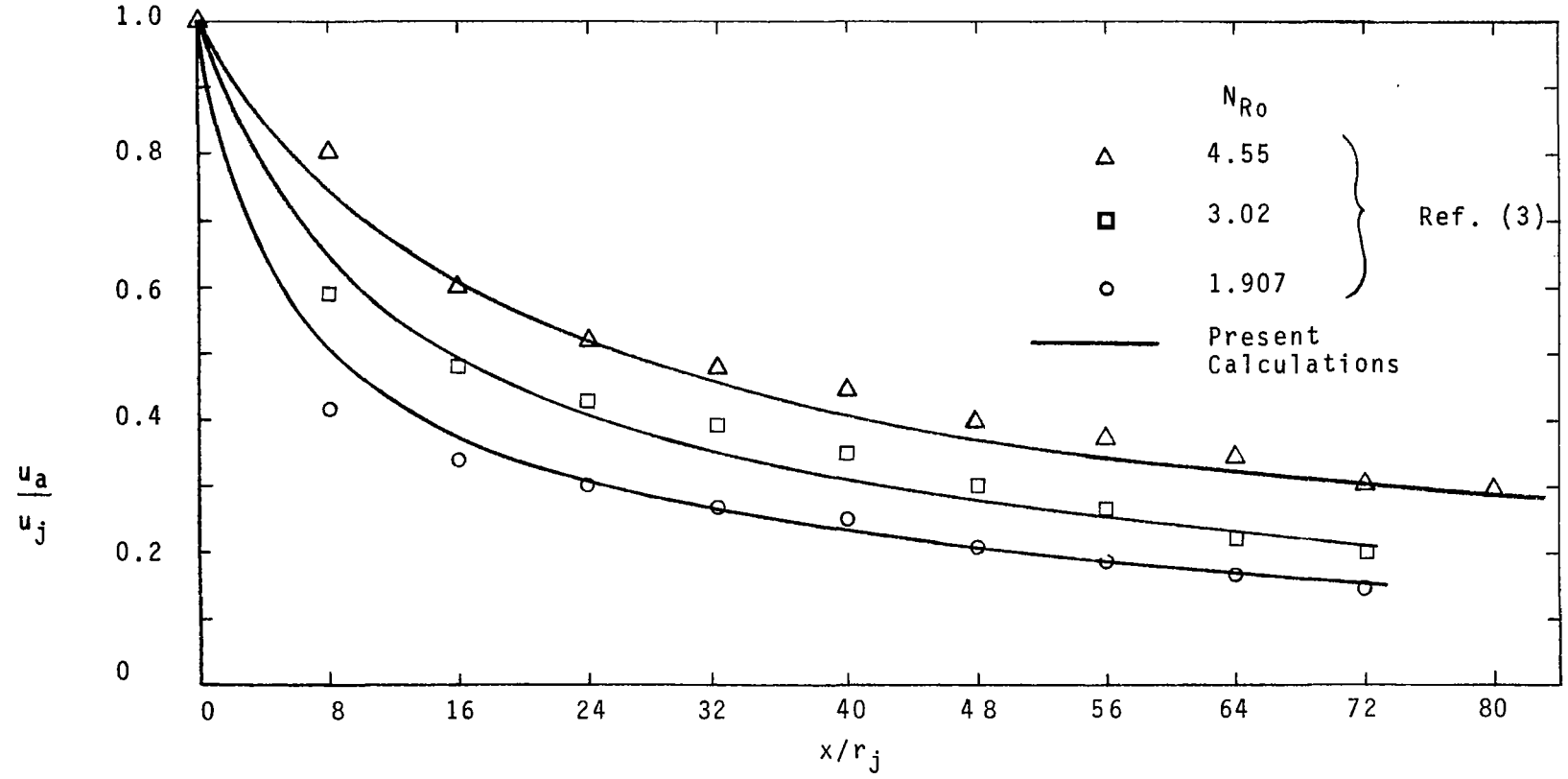

FIGURE 5a. AXIAL VELOCITY DISTRIBUTION ALONG AXIS

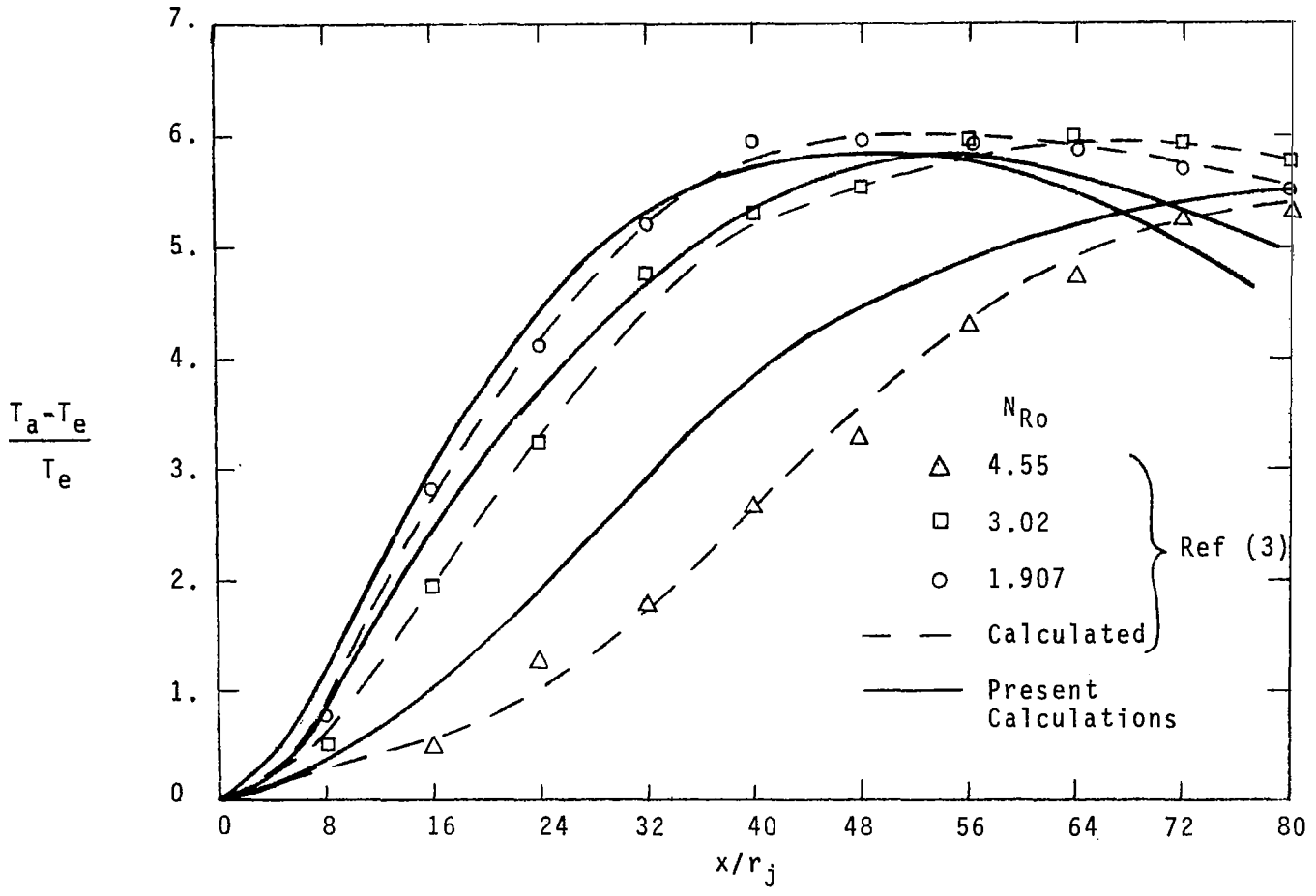

FIGURE 5b. TEMPERATURE DISTRIBUTION ALONG AXIS

to give this agreement. The general tendency for the computed axial temperature to be larger than that observed may imply a breakdown of the flame sheet model in this regime as opposed to an increased Prandtl number.

An interesting observation, in agreement with past analyses is that within a short distance ($x/r_j \sim 15$) the swirl velocity has been reduced to 10% of its original maximum value. Since the swirl correction to the eddy viscosity has been assumed to be a function of the initial conditions and the swirl velocity decays so rapidly, then the usual mixing equations with the equivalent viscosity are sufficient to attain the pertinent free jet results. That is, in the region of low to moderate swirl it is unnecessary to solve the angular momentum and radial equilibrium equations.

To conclude, it appears that an eddy viscosity correction of the order $(1 + 90/N_{RO}^2)^{\frac{1}{2}}$ correlates the few existing free mixing with combustion data in terms of axial temperature and velocity decay as well as flame length.

IV. AN EXAMPLE - DUCTED RING JET COMBUSTION

In this section the preceding results are extended to the analysis of the mixing and combustion of hydrogen injected from a ring jet into a constant area annular air stream. The geometry of this system is given in Figure (6).

The analysis includes the interaction effects of mixing with finite rate chemistry. The introduction of swirl into the fuel jet is examined with respect to its effect on the character of the combustion process. The example chosen is of significance for supersonic combustion where rapid mixing between fuel and air is required.

If the problem is considered to be one of free shear mixing in a confined region (negligible wall boundary layer effects), then the governing equations are similar to those of the free jet discussed previously. In this formulation, however, the energy equation is written in terms of the temperature and chemical species conservation replaces elemental species conservation in order to include the effects of finite rate chemistry in the calculations. Thus,

Conservation of Species Mass

$$\rho u \frac{\partial \alpha_k}{\partial x} + \rho v \frac{\partial \alpha_k}{\partial r} = \frac{1}{r} \frac{\partial}{\partial r} \left(\mu_T \frac{N_{Le}}{N_{Pr}} \quad r \frac{\partial \alpha_k}{\partial r} \right) + \dot{w}_k, \quad k=1,n \qquad (36)$$

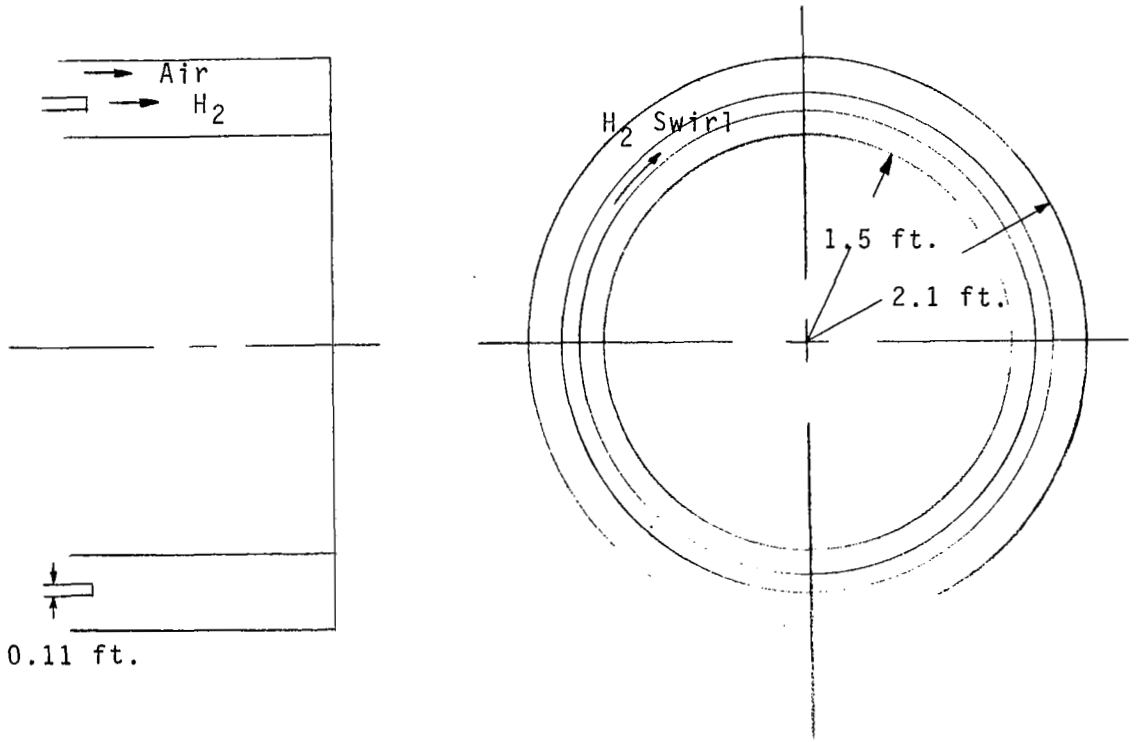

FIGURE 6. SCHEMATIC OF ANNULAR CHAMBER WITH RING INJECTOR

Conservation of Energy

$$\bar{C}_p \rho u \frac{\partial T}{\partial x} + \bar{C}_p \rho v \frac{\partial T}{\partial r} = u \frac{\partial p}{\partial x} + \mu_T \left[\left(\frac{\partial u}{\partial r} \right)^2 + r^2 \left(\frac{\partial}{\partial r} \left\{ \frac{w}{r} \right\} \right)^2 \right]$$

$$- \sum_k \dot{w}_k h_k + \frac{1}{r} \frac{\partial}{\partial r} \left[\frac{\bar{C}_p}{N_{Pr}} \mu_T r \left(\frac{\partial T}{\partial r} - \frac{w^2}{r \bar{C}_p} \right) \right] + \mu_T \frac{N_{Le}}{N_{Pr}} \frac{\partial T}{\partial r} \sum_k C_{p_k} \frac{\partial \alpha_k}{\partial r} \tag{37}$$

The heat conduction term of Equation (37) has been modified by a turbulent heat transfer term that results from the radial pressure gradient, Reference (14). This term accounts for an isentropic expansion and contraction of fluid particles fluctuating between regions of variable pressure. The term is small for the present application but is included for completeness.

As in the free jet case, the equations are more easily handled in von Mises coordinates. The transformation here is

$$\rho u r = \psi \frac{\partial \psi}{\partial r}, \quad \rho v r = - \psi \frac{\partial \psi}{\partial x} \tag{38}$$

where

$$\psi^2 - \psi_i^2 = 2 \int_{r_i}^{r} \rho u r' dr' .$$

Since the coordinate, r, is measured from the origin, the transformation compels the condition $\psi_i \neq 0$ for the inner radius stream function. The value of ψ_i is arbitrary and was eventually chosen in such a way as to enhance the numerical charac-

teristics of the computer program. Application of this transformation results in Equations (28) - (30) given previously and

$$\frac{\partial \alpha_k}{\partial x} = \frac{1}{\psi} \frac{\partial}{\partial \psi}\left(\mu_T \frac{N_{Le}}{N_{Pr}} \frac{\rho u r^2}{\psi} \frac{\partial \alpha_k}{\partial r}\right) + \frac{\dot{w}_k}{\rho u}, \quad k=1,n \tag{39}$$

$$\bar{C}_p \frac{\partial T}{\partial x} = \frac{1}{\rho} \frac{\partial p}{\partial x} + \frac{\rho u r^2}{\psi^2} \mu_T \left[\left(\frac{\partial u}{\partial \psi} \right)^2 + r^2 \left(\frac{\partial w/r}{\partial \psi} \right)^2 \right.$$

$$\left. + \frac{N_{Le}}{N_{Pr}} \frac{\partial T}{\partial \psi} \sum_k C_{p_k} \frac{\partial \alpha_k}{\partial \psi} \right] - \frac{1}{\rho u} \sum_k \dot{w}_k h_k + \frac{1}{\psi} \frac{\partial}{\partial \psi} \left[\mu_T \frac{\bar{C}_{pr}}{N_{Pr}} \left(\frac{\rho u r}{\psi} \frac{\partial T}{\partial \psi} - \frac{w^2}{r \bar{C}_p} \right) \right] \tag{40}$$

for Equations (36) and (37), respectively.

The effects of the walls cannot be directly incorporated into the analysis because of the different length scales involved between the wall boundary layer and free shear layer. Here the latter is the major concern and the effects of the wall are accounted for by using the results of boundary layer theory to obtain a suitable skin friction coefficient, c_f, based upon the absolute velocity. The components of the friction force are assumed to be in proportion to the components of velocity. An a posteriori check showed that the effects of wall shear are negligible in the regime analyzed here. The boundary conditions,

then are given by

$$\text{At} \quad \psi = \psi_i: \quad \frac{\partial \alpha_k}{\partial \psi} = 0, \quad \frac{\partial u}{\partial \psi} = \frac{c_f}{2} \frac{\psi u}{\mu_T r} \left(1 + \frac{w^2}{u^2} \right)^{3/2}$$

$$\frac{\partial w}{\partial \psi} = \frac{w}{u} \frac{\partial u}{\partial \psi}, \quad \frac{\partial T}{\partial \psi} - \frac{\psi w^2}{\rho u r^2 \bar{C}_p} = 0, \quad r = r_i$$

$$\psi = \psi_e: \quad \frac{\partial \alpha_k}{\partial \psi} = 0, \quad \frac{\partial u}{\partial \psi} = - \frac{c_f}{2} \frac{\psi u}{\mu_T r} \left(1 + \frac{w^2}{u^2} \right)^{3/2} \tag{41}$$

$$\frac{\partial w}{\partial \psi} = \frac{w}{u} \frac{\partial u}{\partial \psi}, \quad \frac{\partial T}{\partial \psi} - \frac{\psi w^2}{\rho u r^2 \bar{C}_p} = 0, \quad r = r_e$$

$$x = 0: \quad \alpha_k = \alpha_k(\psi), \quad T = T(\psi), \quad u = u(\psi), \quad w = w(\psi)$$

$$p(0, \psi_i) = P.$$

It is not the purpose of this report to detail the computer programs developed to obtain the results presented herein. The numerical analysis of this problem is similar to that of the free jet and follows the standard techniques for ducted flows, Reference (15), with few modifications.

When no swirl is present the annulus outer wall radius is easily

matched to the outer wall edge stream function by iteration on the axial pressure gradient. All the properties at the next step downstream are calculated based upon an assumed pressure at new axial location. If the value of r calculated at ψ_e is not within 1% of the radial mesh width, then the process is repeated until convergence. When swirl is present, the situation is complicated by a radial pressure gradient. In this case the pressure at the next axial station is assumed only at the inner radius point. The pressure gradient at a point $(\psi+\Delta\psi,x)$ can be related to the pressure at point (ψ,x) by the expansion

$$\left(\frac{\partial p}{\partial x}\right)_{x,\psi+\Delta\psi} = \left(\frac{\partial p}{\partial x}\right)_{x,\psi} + \left(\frac{\partial^2 p}{\partial x \partial \psi}\right)_{x,\psi} \Delta\psi.$$

From Equation (22)

$$\left(\frac{\partial^2 p}{\partial x \partial \psi}\right) = \frac{rw^{\psi}}{ur^4}\left[\frac{2\partial(rw)}{\partial x} - \frac{rw}{u}\frac{\partial u}{\partial x} - \frac{4(rw)}{r}\frac{\partial r}{\partial x}\right]_{\psi,x}$$

so that the radial variation of axial pressure gradient can be estimated at each step. The iteration now procedes in the same manner as for the zero swirl case.

The mixing model is somewhat simplified here. The jet and free stream are both considered, numerically, in the initial plane by assuming initial profiles as a function of stream function. Neglecting the potential core and using the eddy viscosity model

of Equation (15), along with the constants developed in Section III, yields

$$\mu_T = 0.0138 \left[1 + 90(1/\rho)_{avg.} \left(\frac{r_e - r_i}{r_j} \right) \left(\frac{w_{max}\ \rho^{1/2}}{u_{max} - u_{min}} \right)^2 \right]^{1/2} \times \left[(\rho u)_{max} - (\rho u)_{min} \right] (r_e - r_i)$$

$$\text{for } \frac{d}{dr} (\rho r^2 w^2) < 0 \qquad (42)$$

$$\mu_T = 0.0138 \left[(\rho u)_{max} - (\rho u)_{min} \right] (r_e - r_i)$$

$$\text{for } \frac{d}{dr} (\rho r^2 w^2) \geq 0.$$

Here the length scale has been taken as the annulus width and the average specific volume, $(1/\rho)_{avg.}$, is

$$\left(\frac{1}{\rho} \right)_{avg.} = \frac{1}{2} \left[\left(\frac{1}{\rho} \right)_j + \left(\frac{1}{\rho} \right)_e \right] .$$

The model assumes that the effects of swirl are present only in the rotatiorally unstable regime.

Coupling of the chemistry with the fluid dynamics of the system is accomplished by the method of Reference (16). This provides that the one-dimensional chemistry along a streamline may be coupled directly to the two-dimensional mixing equations. The hydrogen-air chemistry that is used here, as well as the two-step subdomain technique used for its computation, are both given in Reference (16).

The flow conditions that are investigated here are

$$
\begin{array}{lll}
N_{Mj} = 1.5 & N_{Me} = 4. & r_i = 1.5 \text{ ft} \\
u_j = 12000 \text{ fps} & u_e = 8700. \text{ fps} & r_e = 2.1 \text{ ft} \\
T_j = 1111. \ ^\circ K & T_e = 1089. \ ^\circ K & \frac{cf}{2} = 0.0025 \\
\Delta r_j = 0.11 \text{ ft} & p(\psi_i, 0) = 2116. \text{ psf} &
\end{array}
\tag{43}
$$

In the first example the ring jet is placed near the center of the annulus width and two cases are presented, one with no swirl and the other with w_j = 3300 fps.

Temperature profiles for these two cases are given in Figure (7a,b). It is seen that the combustion with swirl has taken place faster and more uniformly. The temperature profile with swirl is almost completely uniform at all but the inner radius region after 0.37 ft. Tne inner radius region has characteristics similar to those of the zero swirl case because the assumption has been made that the flow is stable there. This prevents the flame from penetrating the fluid between the injector and the inner wall. Figure (7c,d) depicts the hydrogen species (H_2, H, OH, H_2O) distribution at x=0.37 ft. for the two cases. In particular, the H_2O and H_2 distributions demonstrate that burning is more rapid and uniform for the swirling fuel jet.

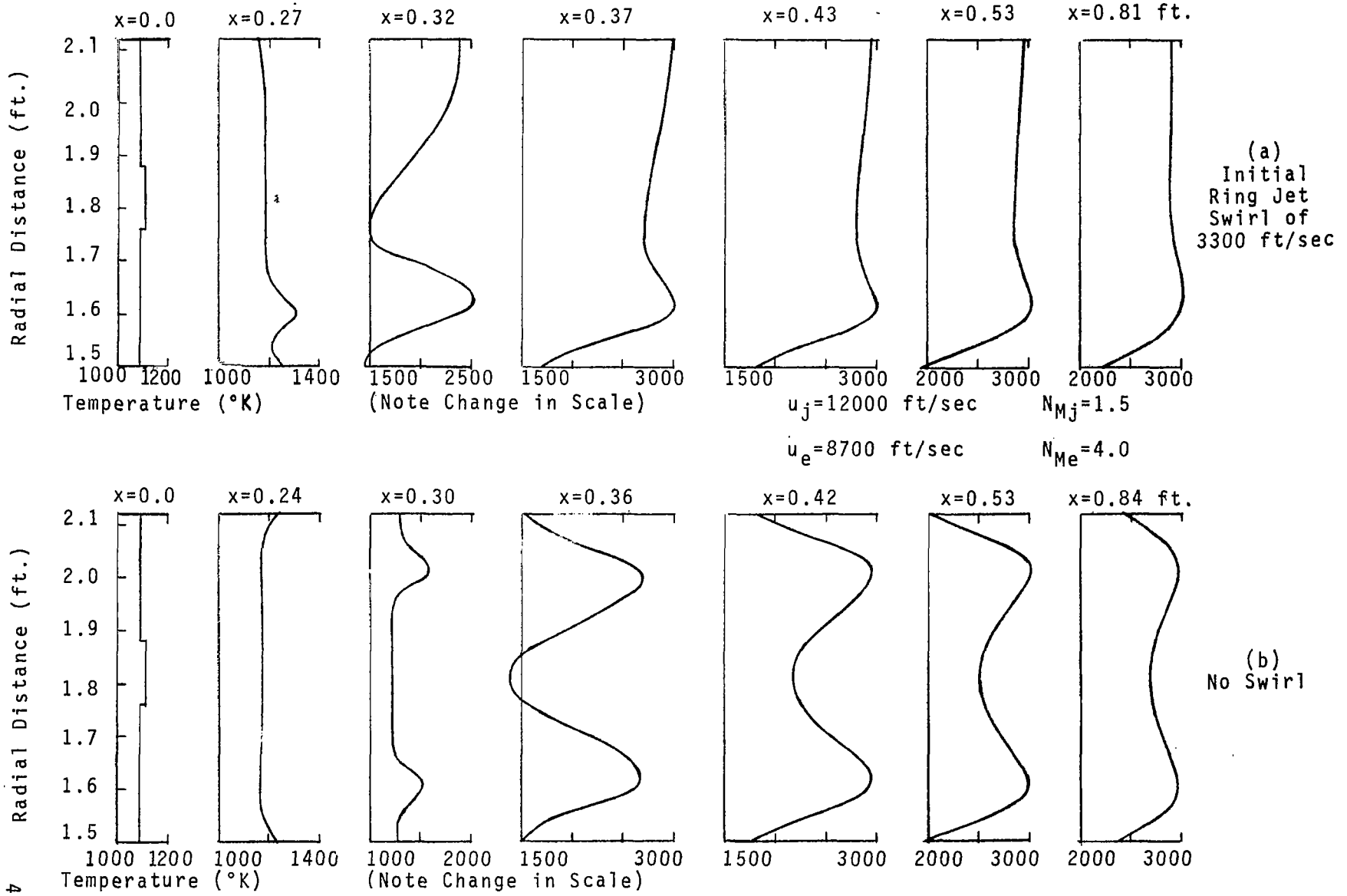

FIGURE 7a,b. TEMPERATURE PROFILES FOR SUPERSONIC COMBUSTION IN AN ANNULUS

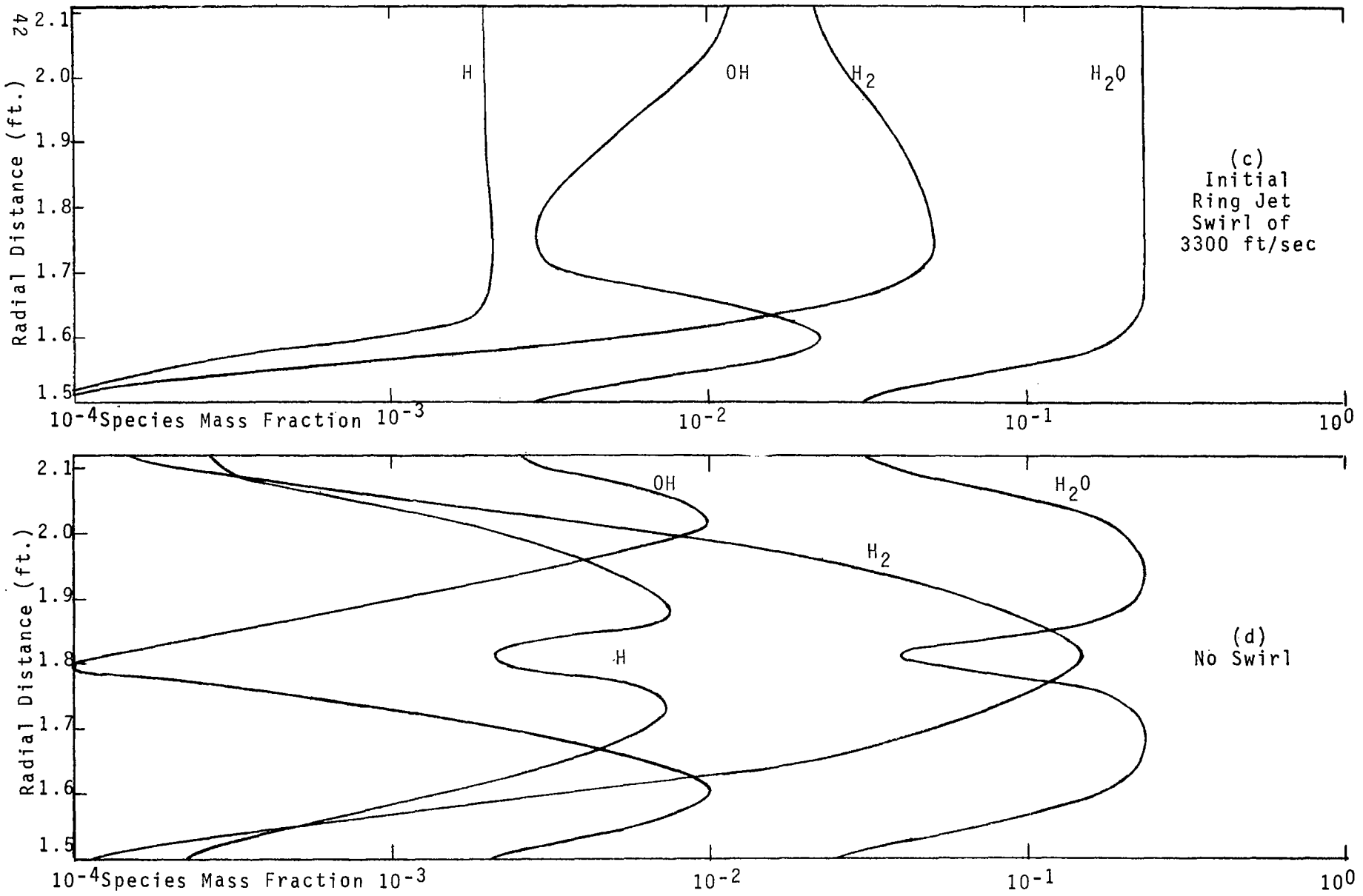

FIGURE 7c,d. HYDROGEN SPECIES MASS FRACTIONS AT x=0.37 FT.

Further indication of the effects of swirl on combustion in the annular channel is given by the inside wall pressure distributions, Figure (8). For the case with swirl, the pressure rise in the channel is limited to a small axial region, similar to a premixed case, indicating that the entire mixture is burned relatively uniformly. The zero swirl case has a gradual increase in the pressure corresponding to a combustion process that is still very much coupled to mixing and where burning is taking place for some distance downstream. The distance for complete combustion appears to have been reduced in half by the addition of swirl to the hydrogen jet.

The combustion with swirl can be made even more uniform by introducing enough swirl to the air between the inner wall and fuel jet to make this region rotationally unstable with respect to the fuel jet. This has the effect of increasing the turbulent transport near the inside wall.

Another method of obtaining better mixing is to locate the fuel jet closer to the inner radius. Since the mixing in the outer region is more rapid than that of the inner region, proper placement of the jet may optimize combustion characterisitics.

A first attempt at this was made by locating the ring jet about 0.2 ft. inside the location of the previous case. In

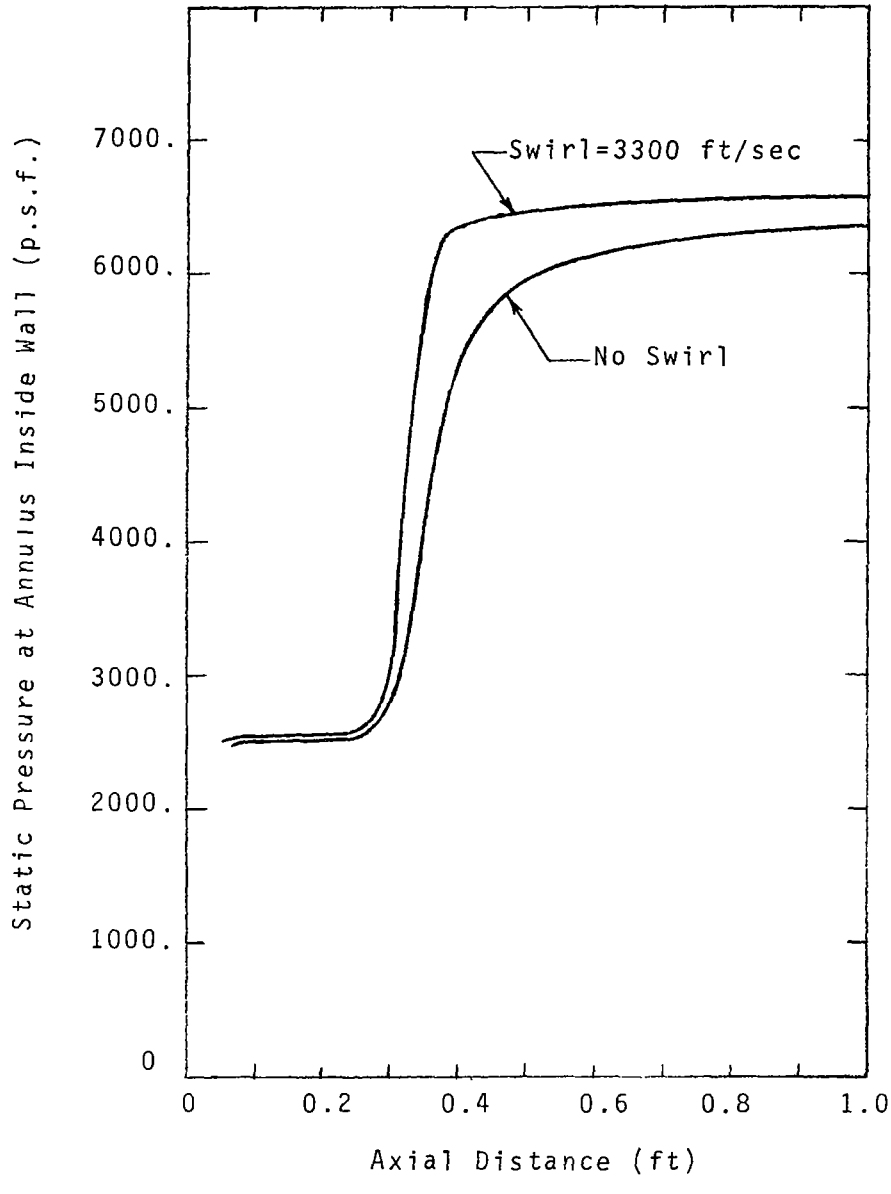

FIGURE 8. PRESSURE DISTRIBUTION IN ANNULUS WITH SUPERSONIC COMBUSTION

Figure (9a) it is seen that this placement may be too near the inside wall since the flame does not reach the outer wall as rapidly as before and the inner wall temperature has been raised very little. This is probably caused by too rich a fuel mixture at the inner wall.

The jet was then placed half way between the location of the two previous cases. In Figure (9b) it can be seen that, although the combustion length has not been reduced, the temperature profile at x=0.83 ft. is now uniform over the entire width of the combustor.

Thus it appears that swirl, along with injector location, can grossly effect the combustion process by altering resulting temperature distributions and the combustion length.

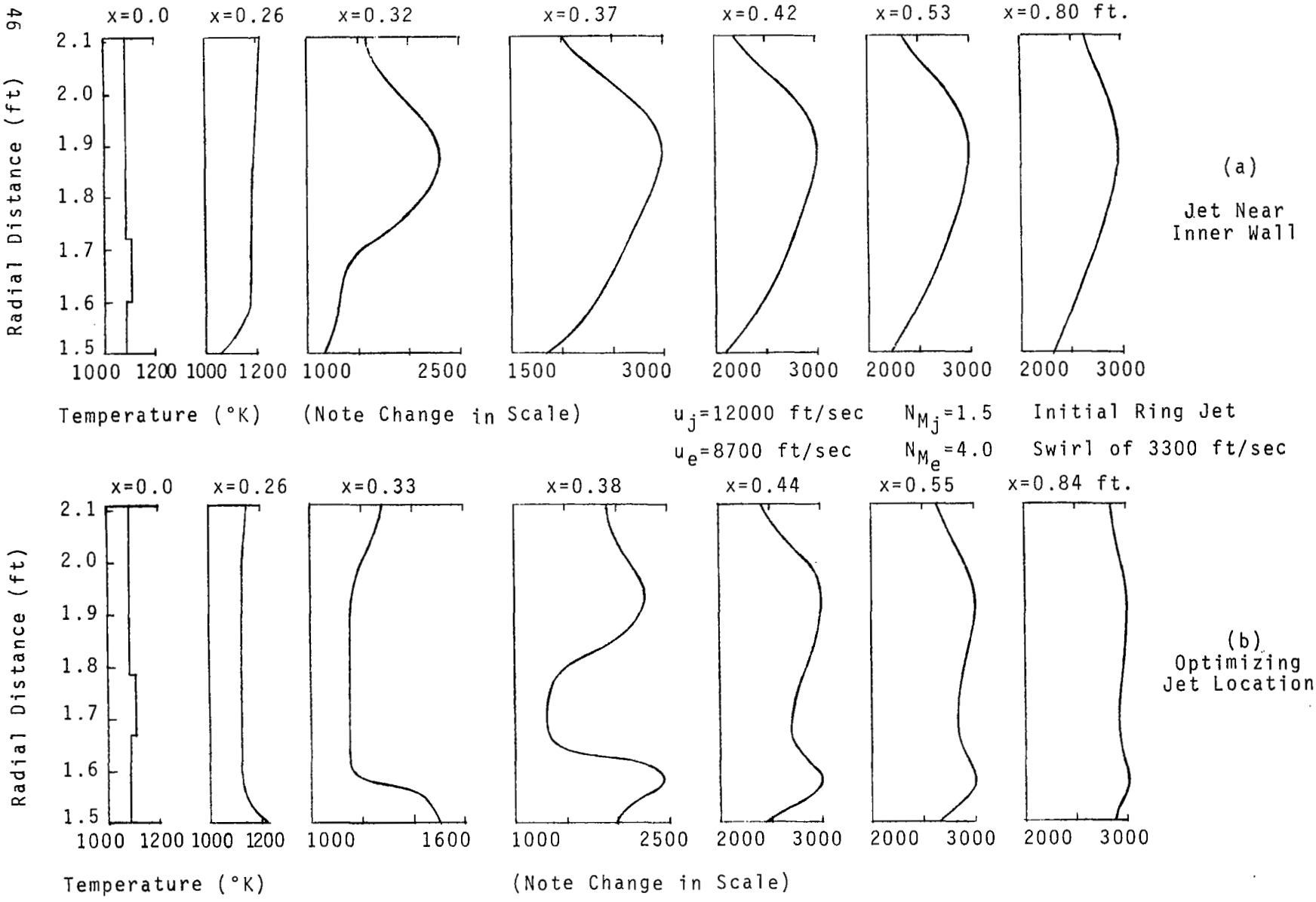

FIGURE 9. EFFECTS OF JET LOCATION ON TEMPERATURE PROFILES

V. CONCLUSIONS

A general formulation of some effects of swirl on turbulent mixing has been given. The basis for the analysis is that momentum transport is enhanced by turbulence resulting from rotational instability of the fluid field.

An appropriate form for the turbulent eddy viscosity is obtained by mixing length type arguments. The result takes the form of a corrective factor that is a function of the swirl and acts to increase the eddy viscosity. The factor is based upon the initial mixing conditions implying that the rotational turbulence decays in a manner similar to that of free shear turbulence.

Existing experimental data for free jet combustion have adequately matched by using the factor $(1 + 90/N_{Ro}^{2})^{\frac{1}{2}}$ to relate the effects of swirl on eddy viscosity.

The model has been extended and applied to the supersonic combustion of a ring jet of hydrogen injected into a constant area annular air stream. The computations demonstrated that swirling the flow could

(1) reduce the burning length by one half

(2) result in more uniform burning across the annulus width

(3) open the possibility of optimization of the combustion characteristics by locating the fuel jet between the inner wall and center of the annulus width.

REFERENCES

1. Schwartz, I. R.; "A Preliminary Investigation of Combustion with Rotating Flow in an Annular Combustion Chamber," NACA RM L51E25a.

2. Niedzwiecki, R. W. and Jones, R. E.; "Combustion Stability of Single Swirl-Can Combustor Modules Using ASTM-A1 Liquid Fuel," NASA TN D-5436, (October, 1969).

3. Chervinsky, A.; "Turbulent Swirling Jet Diffusion Flames," AIAA Journal, 7, 1877-1883, (October, 1969).

4. Rayleigh, Lord; "On the Dynamics of Revolving Fluids," Proc. Roy. Soc. London, A 93, 148-154, (1917).

5. Greenspan, H. P.; "The Theory of Rotating Fluids," Cambridge University Press, (1968).

6. von Kármán, T.; "Some Aspects of the Turbulence Problem," Proc. 4th Intl. Cong. Appl. Mech., Cambridge, 54-59, (1934).

7. Synge, J. L.; "The Stability of Heterogeneous Liquids," Trans. Roy. Soc. Canada, 27, 1-18, (1933).

8. Schlichting, H.; "Boundary Layer Theory," McGraw-Hill Book Company, Inc., 4th Ed., (1960).

9. Chigier, N. A. and Chervinsky, A.; "Experimental and Theoretical Study of Turbulent Swirling Jets Issuing from a Round Orifice," Israel J. of Technology, 4, 44-54, (1966).

10. Chigier, N. A. and Chervinsky, A.; "Aerodynamic Study of Turbulent Burning Free Jets with Swirl," Eleventh Int'l Symp. on Comb., The Combustion Inst., Pittsburgh, pp. 489-499, (1967).

11. Kleinstein, G.; "On the Mixing of Laminar and Turbulent Axially Symmetric Compressible Flows," PIBAL Rep. No. 756, (February, 1963).

12. Ferri, A., Libby, P. A., and Zakkay, V.; "Theoretical and Experimental Investigation of Supersonic Combustion," High Temperatures in Aeronautics, pp. 55-118, Pergamon Press, New York, (1962).

13. Zeiberg, S. and Bleich, G.; "Finite Diference Calculation of Hypersonic Wakes," AIAA Journal, 2, 1936-1404, (1964).

REFERENCES (Continued)

14. Deissler, R. G. and Perlmutter, M.; "Analysis of the Flow and Energy Separation in a Turbulent Vortex," Int. J. Heat Mass Transfer, 1, 173-191, (1960).

15. Edelman, R. and Fortune, O.; "An Analysis of Mixing and Combustion in Ducted Flows," AIAA Paper No. 68-114 (1968).

16. Ferri, A., Moretti, G., and Slutsky, S.; "Mixing Processes in Supersonic Combustion," J. Soc. Ind. Appl. Math. 13, 229-258, (1965).

NASA-Langley, 1972 —— 23 CR-1956